Clement, Romain; Dimnet, Laura; Maberly, Stephen C.; Gontero, Brigitte. 2016. **The nature of the CO2-concentrating mechanisms in a marine diatom, Thalassiosira pseudonana**. *New Phytologist*, 209 (4). 1417-1427. 10.1111/nph.13728

The nature of the CO_2 concentrating mechanisms in a marine diatom, *Thalassiosira pseudonana*.

Romain Clement[a], Laura Dimnet[a], Stephen C. Maberly[b] & Brigitte Gontero[a]

[a]Aix-Marseille Université CNRS, BIP UMR 7281, 31 Chemin Joseph Aiguier, 13402 Marseille Cedex 20, France

[b]Centre for Ecology & Hydrology, Lake Ecosystems Group, Lancaster Environment Centre, Library Avenue, Bailrigg, Lancaster LA1 4AP UK

Corresponding author: Dr B. Gontero

CNRS-BIP, 31 Chemin Joseph Aiguier, 13 402 Marseille Cedex 20 France

Email: bmeunier@imm.cnrs.fr

Phone : 33 4 91 16 45 49

Fax : 33 4 91 16 46 89

Total word count: (< 6500 words)

Introduction (913), Materials and methods (1468), Results (1643), Discussion (1572 words), Acknowledgements (52). SUM = 5648

7 Figures, 2 tables

Summary (194 words)

- Diatoms are widespread in aquatic ecosystems where they may be limited by the supply of inorganic carbon. Their carbon dioxide concentrating mechanisms (CCM) involving transporters and carbonic anhydrases (CAs) are well known, but the contribution of a biochemical CCM involving C4 metabolism is contentious.
- The CCM(s) present in the marine centric diatom, *Thalassiosira pseudonana*, was studied in cells exposed to high or low concentrations of CO_2, using a range of approaches.
- At low CO_2, cells possessed a CCM based on active uptake of CO_2 (70% contribution) and bicarbonate, while at high CO_2, cells were restricted to CO_2. CA was highly and rapidly activated on transfer to low CO_2 and played a key role because inhibition of external CA produced uptake kinetics similar to cells grown at high CO_2. The activities of PEP carboxylase (PEPCase) and the PEP regenerating enzyme, pyruvate phosphate dikinase (PPDK), were lower in cells grown at low than at high CO_2. The ratios of PEPCase and PPDK to ribulose bisphosphate carboxylase were substantially lower than one even at low CO_2.
- Our data suggest that the kinetic properties of this species results from a biophysical CCM and not from C4 type metabolism.

Keywords: Bicarbonate-use, CCM, CO_2, diatom, photosynthesis, *Thalassiosira pseudonana*.

Introduction

Diatoms are unicellular microalgae that appeared around 120 to 250 million years ago (Sims *et al.*, 2006; Sorhannus, 2007) and have since evolved to form a group of 30,000 to 100,000 species (Mann & Vanormelingen, 2013) that are ubiquitous in aquatic and moist habitats. Like other Chromista, diatoms are thought to be derived from endosymbioses between a heterotrophic cell, a red alga, and possibly a genetic contribution from a green alga (Armbrust, 2009; Moustafa *et al.*, 2009; Deschamps & Moreira, 2012). Because of their complex evolutionary history, the diatom genome comprises genes from algae, plus animals and bacteria which confers diatoms with features, such as the presence of the urea cycle, which differentiates them from other photoautotrophs (Allen *et al.*, 2011). This biochemical diversity could be linked to their ecological success since the dominant oceanic phytoplankton switched from cyanobacteria and green algae to Chromista, such as diatoms and haptophytes, (Falkowski *et al.*, 2004) at a time when atmospheric CO_2 concentration declined and O_2 concentration increased (Katz *et al.*, 2005; Armbrust, 2009; Raven *et al.*, 2012). Today, diatoms are responsible for up to 40 % of primary production in the Earth's largest ecosystem, the ocean (Roberts *et al.*, 2007a) and a large proportion of the export of organic carbon to the ocean floor (Sarthou *et al.*, 2005).

Ribulose-1,5-biphosphate carboxylase/oxygenase (Rubisco) is universally present in photosynthetic organisms and catalyses two reactions, a carboxylation of ribulose-1,5-bisphosphate (RuBP) with CO_2, and an oxygenation of RuBP with O_2 (Bowes *et al.*, 1971; Gontero & Salvucci, 2014). These two reactions compete and thus the oxygenase reaction is favoured at low CO_2 concentrations, reducing photosynthesis (Badger *et al.*, 1998). The Michaelis-Menten constant (K_m) for CO_2 of the form 1D Rubisco of diatoms varies from 20 to 60 µM which is higher than the CO_2 concentration in marine ecosystems at equilibrium with the current atmosphere of 400 ppm (~16 µM depending on temperature; (Badger *et al.*, 1998; Whitney *et al.*, 2011)). To circumvent or reduce carbon limitation of photosynthesis, some aquatic photosynthetic organisms, including diatoms, possess Carbon dioxide Concentrating Mechanisms (CCMs) that elevate the CO_2 concentration around Rubisco, thus decreasing the oxygenase reaction and thereby increasing the rate of photosynthesis (Roberts *et al.*, 2007a).

Several types of CCM are known, based on biophysical or biochemical processes. Biophysical CCMs involve active transport of CO_2 or bicarbonate (HCO_3^-), and are present in many diatoms (Matsuda *et al.*, 2011). For instance, in marine diatoms, the SLC4 HCO_3^-

transporter is present in *Phaeodactylum tricornutum* (Nakajima *et al.*, 2013), and homologous encoding genes are also found in *Thalassiosira pseudonana* (Armbrust *et al.*, 2004). Carbonic anhydrase (CA) maintains equilibrium between CO_2 and HCO_3^- by catalysing the reversible interconversion of CO_2 and water into HCO_3^- and protons. It plays a role in diatom CCMs (Hopkinson *et al.*, 2011; Matsuda *et al.*, 2011) and its expression is increased under a low CO_2 concentration in *P. tricornutum* and *T. pseudonana* (Harada *et al.*, 2005; Crawfurd *et al.*, 2011; Hopkinson *et al.*, 2013). In *P. tricornutum*, some CAs are redox-regulated and activated by reduced thioredoxins, suggesting that they are active during the day and inactive at night which is consistent with their participation in a CCM (Kikutani *et al.*, 2012).

Biochemical CCMs involving C4-type photosynthesis have been suggested to be involved in CO_2 assimilation in some diatoms (Reinfelder *et al.*, 2000). A functional C4 CCM requires an additional carboxylation enzyme, typically phosphoenolpyruvate carboxylase (PEPC), that catalyses the carboxylation of phosphoenolpyruvate (PEP) with HCO_3^-, forming a C4 carbon compound. This compound is then cleaved by one of three decarboxylating enzymes to produce CO_2 in the vicinity of Rubisco (Sage, 2004). Although C4 metabolism in terrestrial plants is usually associated with Kranz type anatomy (Sage, 2004), some terrestrial plants, such as *Borszczowia aralocaspica*, perform C4 type photosynthesis within one cell (Voznesenskaya *et al.*, 2001). Similarly, in aquatic environments, *Hydrilla verticillata*, *Ottelia alismoides*, *Egeria densa*, *Udotea flabellum* and *Ulva lynza* are believed to perform this type of photosynthesis without Kranz anatomy (Reiskind & Bowes, 1991; Magnin *et al.*, 1997; Lara *et al.*, 2002; Xu *et al.*, 2013; Zhang *et al.*, 2014) and so it is feasible that this pathway may be present in diatoms (Kroth, 2015).

In two diatoms whose genomes are fully sequenced and annotated, *T. pseudonana* (Armbrust *et al.*, 2004) and *P. tricornutum* (Bowler *et al.*, 2008), all the genes required for C4 type photosynthesis are present. Thus, diatoms have the genetic potential to operate a C4 pathway. However this possibility remains controversial (Raven, 2010) as there are a range of contradictory results for the possession of C4 metabolism in diatoms based on different approaches such as ^{14}C labelling, use of specific C4 enzyme inhibitors (Reinfelder *et al.*, 2004), proteomic analysis, transcriptomic analysis, enzyme localisation and RNA silencing (McGinn & Morel, 2008; Kustka *et al.*, 2014; Tanaka *et al.*, 2014). A recent study (Kustka *et al.*, 2014), however, reaffirmed the operation of C4 photosynthesis in *T. pseudonana* grown at low CO_2 and (Samukawa *et al.*, 2014) concluded that the nature of the CO_2 delivery system to the chloroplast needs to be investigated further (Samukawa *et al.*, 2014).

The aim of this study was therefore to decipher the roles of biophysical and biochemical CCMs in a model diatom, *T. pseudonana*, using a range of techniques. We studied the effect of growth in air (400 ppm CO_2) and extremely high, 20 000 ppm, and low, 50 ppm CO_2, on growth rate, photosynthetic kinetics, the activity of CA and the enzymes involved in C4-type metabolism.

Materials and methods

Strain, media and culture condition

Thalassiosira pseudonana Hasle & Heim., strain CCAP 1085/12 (equivalent to CCMP1335, the strain whose genome has been sequenced), was grown in F/2+Si medium, pH 8, in artificial sea water (mM: 380 NaCl, 3 KCl, 4.39 $CaCl_2$, 1.71 $NaHCO_3$, 20.8 $MgSO_4$, 0.88 $NaNO_3$, 0.036 NaH_2PO_4, 0.11 Na_2SiO_3), trace elements (µM: 12.3 Na_2EDTA, 11.7 $FeCl_3$, 40.1 $CuSO_4$, 0.077 $ZnSO_4$, 0.042 $CoCl_2$, 0.91 $MnCl_2$, 0.013 Na_2Mo_4,) and vitamins (nM: 0.37 B12 (cyanocobalamin), 300 B1 (thiamine-HCl) and 2.05 B8 (biotin)).

Cultures were maintained in a growth cabinet (Innova 4230, New Brunswick Scientific) at 16°C with continuous illumination at 50 µmol photon m^{-2} s^{-1} photosynthetically active radiation (PAR, spectral band 400 to 700 nm) measured with a 2π sensor (Q201, Macam Photometric, Livingstone, UK) and were constantly shaken at 90 rpm. The cultures were aerated with one of three gas mixtures (50, 400 or 20 000 ppm) at a gas flow rate of 130 mL min^{-1} using mass-flow regulators (El-Flow, Bronkhorst High-Tech B.T, Nijverheidsstraat, Netherlands) that mixed air, 2% CO_2 in air, and air that had been passed through soda lime, to remove CO_2 (Intersurgical, Wokingham, UK). Dissolved CO_2 concentrations calculated using equations in (Weiss, 1974) were 2, 16 and 800 µM. Concentrations of CO_2 and other components of the carbonate system were calculated from pH, alkalinity, temperature and salinity using the dissociation constants in Goyet & Poisson (Goyet & Poisson, 1989). During growth experiments, pH was checked daily using a combination pH electrode and meter (Eutech pH 2700, Eutech Instruments, Landsmeer, Netherlands), optical density (OD) was measured at 600 nm using a Perkin Elmer Lambda 25 UV/VIS spectrophotometer (Waltham, MA, USA) and number of cells was counted by microscopy using a Neubauer chamber. Growth rates were calculated as:

$$Growth\ rate = \left(\frac{\ln(y_B) - \ln(y_A)}{x_B - x_A}\right) \quad \text{(Eqn 1)}$$

Where:

$ln(y_B)$ and $ln(y_A)$ correspond to the natural logarithm of OD at 600 nm or cell density (cell mL^{-1}) measured at the start and end of the exponential phase and x_B and x_A correspond to the time (day) of these two points.

Kinetics of O_2 evolution

Rates of net photosynthesis were measured as oxygen evolution in an electrode chamber thermostatted at 16°C (Oxygraph, Hansatech Instruments, Norfolk, UK) using O_2 View software. The chamber was illuminated with a tungsten lamp with a hot-mirror cut-off filter at 750-1100 nm (HMC-1033, UQG Cambridge, UK) to minimise heat input to the chamber. The cells received 200 µmol m^{-2} s^{-1} PAR which preliminary experiments had shown to be saturating but not photo-inhibiting. Cultures from the exponential phase were centrifuged at 3720 g for 10 min at 16°C (Beckman Coulter Allegra® X-15R Centrifuge; rotor: 4750A) and the pellet was rinsed twice, and resuspended in artificial sea water containing 10 mM HEPES at either pH 7 or pH 8. A suspension (1 mL) containing ± 20 million cells was added to the oxygen electrode chamber. Respiration was measured after 10 min in the dark to allow steady-state rates to be produced. The cells were then illuminated and when net oxygen evolution had ceased, small volumes of stock (1, 10 and 100 mM) $NaHCO_3$ were added to produce a range of concentrations of dissolved inorganic carbon (DIC, 10, 20, 50, 100, 150, 200, 500, 1000 and 2000 µM) and the rate of change of oxygen concentration was recorded. To study the effect of CA on the rate of photosynthesis, 0.4 mM (final concentration) of acetazolamide (AZA; Sigma-Aldrich, St Louis, USA) an inhibitor of external CA, was added directly to the oxygen electrode in the light once oxygen evolution had ceased and immediately before the first addition of DIC. Biological duplicates and experimental triplicates were analysed, giving six replicates in total. The response of rate of net photosynthesis to the concentration of DIC was fitted to a slightly modified Michaelis-Menten equation that took into account the compensation point for DIC.

At pH 7, CO_2 represents 8 % of DIC while at pH 8 it only represents 0.8 %. This difference was used to discriminate between the effects of CO_2 and HCO_3^- on net oxygen evolution using a model that assumes separate uptake of these two forms of inorganic carbon with different $K_{½}$ and compensation concentrations but a common total maximum uptake rate:

$$Net\ rate\ of\ photosynthesis = \left(\frac{\alpha * V_{net}^{max} * (CO_2 - CP^C)}{K_{\frac{1}{2}}^C + (CO_2 - CP^C)}\right) + \left(\frac{(1-\alpha) * V_{net}^{max} * (HCO_3^- - CP^B)}{K_{\frac{1}{2}}^B + (HCO_3^- - CP^B)}\right)$$

(Eqn 2)

Where (rate as μmol O_2 mg^{-1} Chl*a* h^{-1} and concentration as μmol L^{-1}):

V_{net}^{max} = the maximum rate of net photosynthesis

α = the proportion of V_{net}^{max} resulting from CO_2 uptake

CO_2 = the concentration of CO_2

CP^C = the CO_2 compensation concentration

$K_{\frac{1}{2}}^C$ = the concentration of CO_2 yielding half-maximal rates of net photosynthesis

HCO_3^- =the concentration of HCO_3^-

CP^B = the HCO_3^- compensation concentration

$K_{\frac{1}{2}}^B$ = the concentration of HCO_3^- yielding half-maximal rates of net photosynthesis

The best fit of the model parameters to the data was obtained by minimising the residual sum of squares of the difference between the measured and modelled rate of net photosynthesis.

Chlorophyll extraction and measurement

The culture was centrifuged at 3720 g, for 10 min at 4°C. The pellet was rinsed in distilled water, re-centrifuged and 2 mL of 96% ethanol was added. After incubation for 15 min at 4°C in the dark, the supernatant was removed and a second extraction was performed. The optical density of the bulked supernatant was measured with the spectrophotometer at 629 and 665 nm. Optical density at 750 nm was negligible and so uncorrected values were used to calculate concentrations of Chlorophyll *a* using the equation in (Ritchie, 2006):

Chl a (μg mL^{-1}) = -1.4014 x A629 + 12.1551 x A665 (Eqn 3)

Protein extraction and content

The soluble protein extracts were prepared following (Erales *et al.*, 2008; Mekhalfi *et al.*, 2014) in a buffer containing 1 mM NAD. The soluble protein concentration of crude extracts

was assayed using the Bio-Rad (Hercules, CA, USA) reagent using bovine serum albumin as a standard (Bradford, 1976).

Enzyme activity measurement

All enzyme activities were measured on cells from the exponential phase of growth. Carbonic anhydrase (CA) activity was measured spectrophotometrically using bromothymol blue as a pH indicator. Crude extracts of cells were incubated in 1.6 mL of buffer (25 mM Tris, 6.4 μM bromothymol blue at pH 9.1) in a cuvette at 3°C. The reaction was started by adding 0.4 mL of CO_2 saturated milliQ water that had been kept on ice. Blanks were performed for each assay by omitting the sample. CA activity was estimated from the time required for the disappearance of the bromothymol blue absorbance at 620 nm which corresponds to a pH decrease from 9.1 to 6.2. Enzyme activity was calculated as Wilbur-Anderson Units (WAU) using the equation (Wilbur & Anderson, 1948):

$$WAU = T_0/T_1 - 1 \quad \text{(Eqn 4)}$$

where T_0 and T_1 correspond to the acidification time without (blank) and with the sample in the reaction mixture, respectively. External CA (eCA) was determined on intact cells; total CA was determined on cells that had been broken by sonicating (Erales *et al.*, 2008); internal CA (iCA) was calculated from the difference between total CA and eCA.

Other enzyme activities were measured from the rate of appearance or disappearance of NADH or NADPH at 340 nm at room temperature (20 to 25ºC). All biochemicals were obtained from Sigma Inc (Saint Louis, MO, USA). PEPC, NAD-dependent malic enzyme (NAD-ME) and Pyruvate phosphate dikinase (PPDK) activities were measured as described previously (Zhang *et al.*, 2014). The activity of fully CO_2-activated and non-activated Rubisco was measured. To activate Rubisco, the extract was pre-incubated in 50 mM Tris, 0.1 mM EDTA, 15 mM $MgCl_2$, 40 mM bicarbonate and 5 mM dithiothreitol pH 8.0 for 10 min prior to assay in a 1 mL cuvette. To measure activity, 5 units of phosphoglycerate kinase and glyceraldehyde-3-phosphate dehydrogenase, 1 mM ATP and 0.2 mM NADH were added and the reaction was started by adding 1 mM ribulose 1,5-bisphosphate. The activity of non-activated Rubisco was measured as above, but the reagents were all added at the same time without pre-incubation. The activation procedure is equivalent to that used to carbamylate Rubisco in higher plants, cyanobacteria and a range of algae but whether or not this is the mechanism involved in activation has not, to our knowledge, been studied in diatoms.

Rubisco, PEPC and CA activities were measured as a function of time after the switch to low CO_2, and the curves were fitted with Sigma Plot software to experimental data using equation 5 for the carboxylases, and their activity ratio and equation 6 for CA:

$$A = A_0 + p(1) * (e^{-p(2)*t}). \quad \text{(Eqn 5)}$$

and

$$A = A_0 + p(1) * (1 - e^{-p(2)*t}) \quad \text{(Eqn 6)}$$

where A is the rate of reaction per mg of Chl*a*, A_0, the activity at the beginning of the experiment before the switch to low CO_2, p(1), the amplitude and p(2), the time constant.

Statistical analysis

Results were analysed using SigmaPlot (v 11.0, Systat Software GmbH, Erkrath, Germany).

Results

Effect of CO_2 on growth rate

The growth rate of *T. pseudonana*, was determined at three concentrations of CO_2. In the absence of algae, pH at equilibrium with 50, 400 and 20 000 ppm CO_2 was 8.8, 7.9 and 6.7. The corresponding calculated CO_2 concentrations were 1, 19 and 320 µM for 50, 400 and 20 000 ppm respectively, which were similar to the theoretical concentrations apart from at the highest CO_2 concentration. In the cultures with algae at 20 000 ppm, the pH dropped quickly to 6.9 and then remained constant for several days (Fig. 1b). During exponential growth, the geometric mean pH was 6.95, equivalent to a CO_2 concentration of about 180 µM. At 400 ppm, pH increased progressively during the exponential phase and reached up to pH 9 to 9.2 at the beginning of the stationary phase. The geometric average pH during the exponential phase was 8.55 which is equivalent to a CO_2 concentration of about 3 µM. Similarly, when the cells were shifted from 20 000 to 50 ppm, the pH also increased and reached over 9.5 corresponding to less than 0.1 µM CO_2 (Fig. 1b). These elevated pH values were caused by the rate of CO_2 consumption at high cell density exceeding the rate of CO_2 supply. The maximum specific growth rate (0.70±0.01 d^{-1}) at 20 000 ppm CO_2 was about 1.3-fold higher than at 400 ppm CO_2 (0.54±0.02 d^{-1}, Fig. 1a). A similar ratio of growth rate at high and air CO_2 was found, based on cell counts (data not shown). *T. pseudonana* was unable to grow when transferred from 20 000 to 50 ppm (Fig. 1a). Since the pH in the 50 ppm treatment was

stable for several days, it indicates that the treatment was not so severe as to cause cell death and this is consistent with the optical density data (Fig. 1a).

Photosynthetic activity

The maximal rate of net photosynthesis (V_{net}^{max}) of *T. pseudonana* grown under 400 ppm CO_2 and measured at pH 7 (*ca* 110 µmol O_2 h^{-1} mg^{-1} Chl*a*) was similar to that measured at pH 8 (Fig. 2a, Table 1). In contrast, the half-saturation concentration for DIC at pH 7 was about 3-fold lower than that at pH 8 (Table 1). The DIC compensation point was also 3-fold lower at pH 7 than at pH 8. For cells grown at 20 000 ppm CO_2, the maximal photosynthetic activity (V_{net}^{max}) measured at pH 7 was *ca* 205 µmol O_2 h^{-1} mg^{-1} Chl*a* which was twice that measured at pH 8 (Fig. 2d, Table 1). The half-saturation concentrations for DIC at pH 7 and pH 8, in contrast, were rather similar and around 50 µM. The DIC compensation points were 3 and 5 µM at the two pH values. When *T. pseudonana* was grown at 20 000 ppm CO_2, the slope of rate of photosynthesis against DIC was between 3.5 and 6.5-fold lower than that found when *T. pseudonana* was grown at 400 ppm CO_2 (Table 1).

The different kinetic parameters at pH 7 and 8 are consistent with different proportions of CO_2 and HCO_3^- being present at these two pH values and we used this to develop a model that distinguished between CO_2 and HCO_3^- uptake (Eqn 2). For cells grown at 400 ppm, this model gave a good fit to the data (R^2 of 0.92; Table 2) and a V_{net}^{max} of 112 µmol O_2 h^{-1} mg^{-1} Chl*a*, corresponding to the sum of CO_2- and HCO_3^--dependent uptake, that was similar to that found when modelling kinetics against DIC. The model predicted that at saturation, CO_2 contributed 70% and HCO_3^- contributed 30% to the maximal rate (Fig. 2b, c). The half-saturation concentration for CO_2 was 0.4 µM which was 7.5-fold lower than that for HCO_3^- at 3 µM. The compensation points were close to 0 for CO_2 and 7 µM for HCO_3^-. The slope of uptake was 7-times higher for CO_2 than for HCO_3^-.

For cells grown at 20 000 ppm, the model gave a less good fit to the data than at 400 ppm (R^2 of 0.60; Table 2). The V_{net}^{max} for CO_2 was nearly identical to that of DIC and the contribution of HCO_3^- was zero (Fig. 2e, f, Table 2). The half-saturation concentration for CO_2 was 3.8 µM. and the compensation point was again close to 0 for CO_2. In comparison to the cells grown at 400 ppm, cells at 20 000 ppm had a 1.8-fold greater V_{net}^{max}, a nearly 10-fold higher half-saturation constant for CO_2, and thereby a 5.5-fold lower slope against CO_2 and lacked the ability to use HCO_3^-. At ambient conditions, presumed to be 16 µM CO_2 and 2000 µM HCO_3^-, the rate of net photosynthesis was 98% saturated for cells grown at 400 ppm but

only 80% saturated for cells grown at 20 000 ppm (Table 2). For a 10-times lower CO_2 concentration of 1.6 µM, the rate of net photosynthesis was 81% and 30% saturated for cells grown at 400 and 20 000 ppm, respectively. Ambient concentrations of 2000 µM HCO_3^- were saturating for cells grown at 400 ppm but HCO_3^- use was absent in cells grown at 20 000 ppm.

Net photosynthetic rate was also measured at pH 7 for cells switched from 20 000 ppm CO_2 to low CO_2 (50 ppm) for 6 h or 12 h (Fig. 3). After 6 h or 12 h at a low CO_2 concentration, the slopes were lower than that of cells grown at 400 ppm CO_2 concentration. However at pH 7, V_{net}^{max} values were intermediate to those found at 400 and 20 000 ppm, with a tendency to decrease as a function of time (Table 1). The half-saturation constant values also decreased as a function of time (Table 1). However, even after twelve hours at 50 ppm, the slope of photosynthesis rate to concentration of DIC was lower than for cells grown for several days at 400 ppm.

Enzyme activities

Enzymes that could be involved in biochemical or biophysical CCMs in *T. pseudonana* were studied. The activity of Rubisco was lower in cells grown at 400 ppm, compared to 20 000 ppm (1.59-fold, Student t-test $p< 0.001$; Fig. 4). The rates of Rubisco activity (as carbon) cannot account for the oxygen-based rates of photosynthesis (6 *vs* 100 µmol.h^{-1}.mg^{-1} Chl*a* at 400 ppm and 20 *vs* 205 µmol.h^{-1}.mg^{-1} Chl*a* at 20 000 ppm). The activity of fully CO_2-activated Rubisco was however about 3-fold higher than that of non-activated enzyme both at 400 (18 µmol.h^{-1}.mg^{-1} Chl*a*) and 20 000 ppm CO_2 (60 µmol.h^{-1}.mg^{-1} Chl*a*) but again this was lower than the oxygen-based rates of photosynthesis even after assuming a photosynthetic quotient of 1.26 (Spilling *et al.*, 2015). However, other mechanisms such as activation by protein-protein interaction with for instance, CbbX may also be involved (Mueller-Cajar *et al.*, 2011). Surprisingly activities of the C4 enzymes, PEPC and PPDK were also lower (5.3-fold, Student t-test $p< 0.001$; 4.6-fold, Student t-test $p< 0.001$ for PEPC and PPDK respectively) in cells from 400 ppm than those from 20 000 ppm CO_2. In contrast, in cells grown at 400 ppm, NAD-ME and CA activities were higher (4.3-fold, Student t-test $p< 0.001$ and 3.75-fold, Student t-test $p< 0.001$, respectively) than in cells grown at 20 000 ppm CO_2.

T. pseudonana cells acclimated to 20 000 ppm CO_2 were shifted to 50 ppm CO_2 to determine the rate of acclimation and to characterize the CCM under more carbon limiting conditions. Rubisco and PEPC activities both decreased exponentially with a time constant of 0.086 (0.044) and 0.064 (0.035) h^{-1}, respectively (Fig. 5a). Consequently, the PEPC:Rubisco

ratio, which began at about 0.27, also decreased exponentially to reach about 0.07, 48 h after the switch to low CO_2 (Fig. 5b). Therefore the PEPC: Rubisco ratios are always much lower than 1. Twelve hours after the switch to 50 ppm CO_2, the activity of NAD-ME increased 5.6 (1.2)-fold while that of PPDK decreased 2.4 (0.2)-fold. These data therefore do not support a role for C4 type photosynthesis in the carbon assimilation of *T. pseudonana.*

In contrast, upon the switch to low CO_2 concentration, CA activity was induced rapidly. The CA activity that was less than 300 WAU increased exponentially to reach a modelled value of 4890 (700) WAU (16-fold increase) with a time constant of 0.13 (0.0587) h^{-1} (Fig. 5c). A ratio between internal CA (iCA) and external CA (eCA) of approximately 1 was obtained for cells grown at all three CO_2 concentrations. The effect of inhibiting eCA on the net photosynthetic rate of the cells grown at 400 ppm CO_2 was tested at pH 7 using a specific inhibitor of eCA, AZA. The addition of AZA increased the half-saturation constant for DIC 5-fold, increased the compensation point about 3-fold and decreased the slope of response to DIC 4-fold but did not affect the maximum rate of net photosynthesis (Fig. 6, Table 1). The kinetic response of cells grown at 400 ppm CO_2 but treated with AZA resembled those grown at 20 000 ppm CO_2 (Table 1) suggesting that eCA has a key role in the carbon uptake properties in *T. pseudonana.*

In order to check if the response to low CO_2 was reversed on return to high CO_2, cultures grown at 20 000 ppm, switched to 50 ppm for 24 h were then switched back to 20 000 ppm for 12 h. While PEPC and PPDK activity increased (by 4.5-fold, Student t-test $p<0.001$ and 5.3-fold, Student t-test $p<0.001$, respectively), Rubisco activity did not change. NAD-ME and CA activity decreased (1.4-fold, Student t-test $p< 0.05$ and 3.3-fold Student t-test $p<0.001$, respectively) (Fig. 7).

These results show that the responses of *T. pseudonana* to CO_2 are rapid and reversible. The kinetic properties of carbon uptake are strongly linked to the activity of CA, and the enzyme activity profiles suggest that carbon fixation involves C3 rather than C4 metabolism.

Discussion

Biophysical CCM in *T. pseudonana*

Cells grown at 400 ppm CO_2 have a $K_{1/2}$ for CO_2 of only 0.4 µM, which is in good agreement with the growth $K_{½}$ estimated for *T. pseudonana* (Clark & Flynn, 2000) at 273 µM DIC, equivalent to about 1.4 µM CO_2 under their experimental conditions. Both estimates are substantially lower than the $K_{1/2}$ for diatom 1D Rubisco (20 to 60 µM) (Whitney *et al.*, 2011) which clearly indicates that some form of CCM is operating. *T. pseudonana* grown at 400 ppm CO_2 preferentially used CO_2 (70 %) rather than HCO_3^- (30 %) at ambient and saturating conditions despite the approximately 120-fold higher concentration of HCO_3^-. This is similar to *P. tricornutum* (Burkhardt *et al.*, 2001) but different from *T. weissflogii* which took up CO_2 and HCO_3^- at a similar rate (Burkhardt *et al.*, 2001). For cells grown at 400 ppm, our reported $K_{½}$ for DIC at pH 8 and 16°C, is very similar to that obtained for the same species at pH 8.2 and 20°C (Nakajima *et al.*, 2013) and to that reported for low CO_2-grown *Chlamydomonas reinhardtii* cells (Sültemeyer *et al.*, 1988).

Cells of *T. pseudonana* grown at a 20,000 ppm CO_2 were only able to use CO_2 and the affinity ($K_{1/2}$) for DIC was over 5-fold lower than for cells grown at 400 ppm CO_2, a down-regulation that has been reported in this and other marine diatoms e.g. (Burkhardt *et al.*, 2001; Trimborn *et al.*, 2009; Nakajima *et al.*, 2013)and *C. reinhardtii* (Sültemeyer *et al.*, 1988). In *T. pseudonana*, the $K_{1/2}$ for CO_2 was still about 4 µM and so substantially lower than the $K_{1/2}$ value for Rubisco: some down-regulated form of CCM therefore, still seems to be operating in *T. pseudonana* grown at 20 000 ppm. External and internal CA activity was also still present in these cells which might be adequate to promote CO_2 uptake which is consistent with the finding that some forms of CA are constitutive in this species (Samukawa *et al.*, 2014).

CA appears to be crucial in this CCM and that of other marine diatoms (Hopkinson *et al.*, 2011). Our enzymatic activity data showing a rapid 4-fold up-regulation at 400 compared to 20,000 ppm are similar to previous reports (Hopkinson *et al.*, 2013) and also in agreement with data obtained at the transcriptional level (McGinn & Morel, 2008; Kustka *et al.*, 2014; Samukawa *et al.*, 2014). All these reports indicate an increase in CA under low CO_2. In *T. pseudonana*, CA is present in the periplasmic space, cytosol, mitochondria, periplastidial compartment and stroma (Tanaka *et al.*, 2005; Samukawa *et al.*, 2014). Using AZA we observed a decreased affinity for DIC, with kinetics very similar to those of cells growing at 20 000 ppm, underlining the important role that extracellular CA plays in this CCM. So far as

we are aware, there is no literature for aquatic (or terrestrial) photoautotrophs with C4 metabolism relying on eCA. On the contrary, work by Reiskind, Seamon & Bowes (Reiskind *et al.*, 1988) on the CCM in the marine green macroalgae *Udotea flabellum,* which has a C4 fixation pathway based on phosphoenolpyruvate carboxykinase, showed that CA was not involved since the CCM was active in the presence of a CA inhibitor. Furthermore, although the model of Kustka et al. (2014) reported upregulation of a number of carbonic anhydrases, including CA-6 that could be located at the cell surface, in their model (Fig. 6) they located it in the chloroplast endoplasmic reticulum. However, although there is no experimental evidence for eCA being involved in C4 metabolism, and most interpretations of CA increases are linked to the operation of a biophysical CCM, it is theoretically possible that an eCA could facilitate the rate of inward-diffusion of either CO_2 or HCO_3^- or both.

As has been found for higher plant Rubisco (Lorimer *et al.*, 1976), we observed an increase of Rubisco activity upon CO_2-activation, presumably linked to a change in Rubisco carbamylation state, which was 3-fold for cells grown at 400 and 20 000 ppm CO_2. Rubisco activity, whether the enzyme was activated or not, was always higher at high *vs* low CO_2, on a Chl*a* basis. It is possible that the greater Rubisco activity at high CO_2 increased the capacity to fix CO_2, since there appears to be little excess carboxylation capacity in diatoms (Glover & Morris, 1979).

Evidence for and against C4 metabolism in *T. pseudonana*

Whether or not C4 photosynthesis is involved in any of the kinetic characteristics that have been observed in *T. pseudonana* has been a matter of debate. Kutska *et al.* (Kustka *et al.*, 2014) produced a model of C4 metabolism for *T. pseudonana* in which PEPC, in the chloroplastic endoplasmic reticulum or the periplastidic space, fixes HCO_3^- to produce oxaloacetic acid that is transported to the chloroplast where it is decarboxylated by pyruvate carboxylase to produce CO_2 in the vicinity of Rubisco.

In our experiments, the activity of PEPC was lower in cells from low CO_2 (grown at 400 or switched to 50 ppm) compared to high CO_2 (20 000 ppm): the opposite to what is expected for C4 metabolism. The ratio of PEPC:Rubisco was also lower at 400 compared to 20 000 ppm and decreased with time when cells were switched from 20 000 to 50 ppm. Furthermore, the ratio of PEPC:Rubisco in *T. pseudonana* was always much less than one while in aquatic C4 plants this ratio is between 1.8 and 6.6 and, in terrestrial plants, it is more than five (Zhang *et al.*, 2014). Moreover, the activity of other enzymes required for the operation of the C4 cycle, such as PPDK, was also lower at low CO_2. Although NAD-ME,

one of the three possible decarboxylating C4 enzymes, had a 4-fold higher activity at 400 compared to 20 000 ppm, this enzyme also contributes to the overall regulation of malate metabolism in many organisms and thus its increase in activity is not necessarily associated with C4 metabolism. Malate is an important substrate for mitochondria, and a significant fraction of glycolytic products enters the Krebs cycle via the combined action of PEPCase, malate dehydrogenase, and malic enzyme without any link to C4 metabolism. Recently it has been shown that NAD-ME is located within the mitochondria in *P. tricornutum*, (Xue *et al.*, 2015) and within the cytosol in *T. pseudonana* (Tanaka *et al.*, 2014). This suggests that the CO_2 released from this decarboxylation would not be in the vicinity of Rubisco. Overall, these enzyme activities, and their pattern of change, are inconsistent with the operation of C4 photosynthesis in this species.

The conclusion that C4 metabolism is not an important component of the CCM in *T. pseudonana* is in agreement with recent work of (Tanaka *et al.*, 2014) who observed a greater abundance of PEPC1 and PEPC2 transcripts in high, compared to low, CO_2. Similarly, the transcripts for other enzymes potentially involved in C4 photosynthesis, PEPCK, PPDK and NAD-ME, were not higher when *T. pseudonana* was grown in low compared to high CO_2, nor were they regulated by the circadian cycle suggesting they are not involved in C4 photosynthesis. The absence of C4 metabolism was also concluded from the lack of change in PEPC:Rubisco ratio in cells of *T. pseudonana* grown at 50 or 800 ppm (Trimborn *et al.*, 2009). Finally, pulse-chase experiments showed that *T. pseudonana* did not incorporate 4-carbon molecules during photosynthesis and immunoblots showed no difference in PEPC abundance in cells grown at 380 or 100 ppm (Roberts *et al.*, 2007b). In contrast, the addition of 3,3-dichloro-2-(dihydroxyphosphinoylmethyl)-propenoate (DCDP), an inhibitor of PEPC, or 3-mercaptopicolinic acid (3-MPA) an inhibitor of PEPCK, reduced photosynthetic activity in *T. pseudonana* (McGinn & Morel, 2008). However, it has subsequently been shown that both inhibitors had no effect on the half-saturation constant but instead inhibited V_{max} suggesting that they had a general toxic effect on metabolism rather than a specific effect on the CCM (Tanaka *et al.*, 2005; Tanaka *et al.*, 2014). The reason for these different conclusions is currently unclear. Kustka *et al.*, (2014) reported rapid (within 30 minutes) but transient (returned close to pre-transient levels in 90 minutes) changes in two forms of PEPC transcripts on transfer from pH 7.61 to 8.48. An alternative explanation to PEPC playing a photosynthetic role is that the response is linked to internal pH homeostasis by the production of carboxylic acids. Haimovich-Dayan *et al.* (2013) concluded that *P. tricornutum* lacked C4

metabolism and proposed that any C4-like metabolism is a futile cycle to dissipate light energy rather than to fix carbon and may also play a role in internal pH homeostasis (Haimovich-Dayan *et al.*, 2013). Although diatoms such as *T. pseudonana* have biophysical pH regulation mechanisms based on a Na^+-energised plasmalemma (Taylor *et al.*, 2012), a biochemical pH-stat based on PEPC as part of the glycolytic pathway may also be involved in pH regulation (Sakano, 1998). The steady-state up-regulation of PEPC reported by Kustka *et al.* (2014) of between 1.52- and 1.75-fold is much lower than for the different forms of CA whose protein-level up-regulation is in broad agreement with our changes in activity. Kustka *et al.* (2014) also reported an up-regulation of two forms of the anion channel Bestrophin (Hartzell *et al.*, 2008) of between 3.31- and 4.24-fold which could be involved in facilitating diffusion of oxaloacetate into the chloroplast. However, Bestrophin can also act as a HCO_3^- channel (Qu & Hartzell, 2008) which would also be consistent with a biophysically based CCM.

Acknowledgements

RC's studentship was supported by the Ministère de l'Education Nationale, de la Recherche et de la Technologie (MENRT). Financial support was provided by CNRS, Aix Marseille Université, the Region PACA, IBiSA and A*MIDEX project (n° ANR-11-IDEX-0001-02) (BG) and the UK Natural Environment Research Council (SCM). We thank Ahmed Zellat for technical support.

Author Contribution

RC, SM and BG planned and designed the research. RC and LD performed the experiments. RC, SM and BG analyzed the data and wrote the manuscript.

References

Allen AE, Dupont CL, Obornik M, Horak A, Nunes-Nesi A, McCrow JP, Zheng H, Johnson DA, Hu H, Fernie AR, et al. 2011. Evolution and metabolic significance of the urea cycle in photosynthetic diatoms. *Nature* **473**(7346): 203-207.

Armbrust EV. 2009. The life of diatoms in the world's oceans. *Nature* **459**(7244): 185-192.

Armbrust EV, Berges JA, Bowler C, Green BR, Martinez D, Putnam NH, Zhou S, Allen AE, Apt KE, Bechner M, et al. 2004. The genome of the diatom *Thalassiosira pseudonana*: ecology, evolution, and metabolism. *Science* **306**(5693): 79-86.

Badger MR, Andrews TJ, Whitney SM, Ludwig M, Yellowlees DC, Leggat W, Price GD. 1998. The diversity and coevolution of Rubisco, plastids, pyrenoids, and chloroplast-based CO_2-concentrating mechanisms in algae. *Canadian Journal of Botany* **76**(6): 1052-1071.

Bowes G, Ogren WL, Hageman RH. 1971. Phosphoglycolate production catalyzed by ribulose diphosphate carboxylase. *Biochemical and Biophysical Research Communications* **45**(3): 716-722.

Bowler C, Allen AE, Badger JH, Grimwood J, Jabbari K, Kuo A, Maheswari U, Martens C, Maumus F, Otillar RP, et al. 2008. The *Phaeodactylum* genome reveals the evolutionary history of diatom genomes. *Nature* **456**(7219): 239-244.

Bradford MM. 1976. A rapid and sensitive method for the quantitation of microgram quantities of protein utilizing the principle of protein-dye binding. *Analytical Biochemistry* **72**(1–2): 248-254.

Burkhardt S, Amoroso G, Riebesell U, Sültemeyer D. 2001. CO_2 and HCO_3^- uptake in marine diatoms acclimated to different CO_2 concentrations. *Limnology and Oceanography* **46**(6): 1378-1391.

Clark DR, Flynn KJ. 2000. The relationship between the dissolved inorganic carbon concentration and growth rate in marine phytoplankton. *Proc Biol Sci* **267**(1447): 953-959.

Crawfurd KJ, Raven JA, Wheeler GL, Baxter EJ, Joint I. 2011. The response of *Thalassiosira pseudonana* to long-term exposure to increased CO_2 and decreased pH. *PLoS ONE* **6**(10): e26695.

Deschamps P, Moreira D. 2012. Reevaluating the green contribution to diatom genomes. *Genome Biology and Evolution* **4**(7): 795-800.

Erales J, Gontero B, Maberly SC. 2008. Specificity and function of glyceraldehyde-3-phosphate dehydrogenase in a freshwater diatom, *Asterionella formosa* (Bacillariophyceae). *Journal of Phycology* **44**(6): 1455-1464.

Falkowski PG, Katz ME, Knoll AH, Quigg A, Raven JA, Schofield O, Taylor FJR. 2004. The evolution of modern eukaryotic phytoplankton. *Science* **305**(5682): 354-360.

Glover HE, Morris I. 1979. Photosynthetic carboxylating enzymes in marine phytoplankton. *Limnology and Oceanography* **24**(3): 510-519.

Gontero B, Salvucci ME. 2014. Regulation of photosynthetic carbon metabolism in aquatic and terrestrial organisms by Rubisco activase, redox-modulation and CP12. *Aquatic Botany* **118**(1): 14-23.

Goyet C, Poisson A. 1989. New determination of carbonic acid dissociation constants in seawater as a function of temperature and salinity. *Deep Sea Research Part A. Oceanographic Research Papers* **36**(11): 1635-1654.

Haimovich-Dayan M, Garfinkel N, Ewe D, Marcus Y, Gruber A, Wagner H, Kroth PG, Kaplan A. 2013. The role of C4 metabolism in the marine diatom *Phaeodactylum tricornutum*. *New Phytologist* **197**(1): 177-185.

Harada H, Nakatsuma D, Ishida M, Matsuda Y. 2005. Regulation of the expression of intracellular beta-carbonic anhydrase in response to CO_2 and light in the marine diatom *Phaeodactylum tricornutum*. *Plant Physiology* **139**(2): 1041-1050.

Hartzell HC, Qu Z, Yu K, Xiao Q, Chien L-T. 2008. Molecular physiology of bestrophins: Multifunctional membrane proteins linked to best disease and other retinopathies. *Physiological Reviews* **88**(2): 639-672.

Hopkinson BM, Dupont CL, Allen AE, Morel FMM. 2011. Efficiency of the CO_2-concentrating mechanism of diatoms. *Proceedings of the National Academy of Sciences* **108**(10): 3830-3837.

Hopkinson BM, Meile C, Shen C. 2013. Quantification of extracellular carbonic anhydrase activity in two marine diatoms and investigation of its role. *Plant Physiology* **162**(2): 1142-1152.

Katz ME, Wright JD, Miller KG, Cramer BS, Fennel K, Falkowski PG. 2005. Biological overprint of the geological carbon cycle. *Marine Geology* **217**(3–4): 323-338.

Kikutani S, Tanaka R, Yamazaki Y, Hara S, Hisabori T, Kroth PG, Matsuda Y. 2012. Redox regulation of carbonic anhydrases via thioredoxin in chloroplast of the marine diatom *Phaeodactylum tricornutum*. *Journal of Biological Chemistry* **287**(24): 20689-20700.

Kroth PG. 2015. The biodiversity of carbon assimilation. *Journal of Plant Physiology* **172**(0): 76-81.

Kustka AB, Milligan AJ, Zheng H, New AM, Gates C, Bidle KD, Reinfelder JR. 2014. Low CO_2 results in a rearrangement of carbon metabolism to support C4 photosynthetic carbon assimilation in *Thalassiosira pseudonana*. *New Phytologist* **204**(3): 507-520.

Lara MV, Casati P, Andreo CS. 2002. CO_2-concentrating mechanisms in *Egeria densa*, a submersed aquatic plant. *Physiologia Plantarum* **115**(4): 487-495.

Lorimer GH, Badger MR, Andrews TJ. 1976. The activation of ribulose-1,5-bisphosphate carboxylase by carbon dioxide and magnesium ions. Equilibria, kinetics, a suggested mechanism, and physiological implications. *Biochemistry* **15**(3): 529-536.

Magnin NC, Cooley BA, Reiskind JB, Bowes G. 1997. Regulation and localization of key enzymes during the Induction of Kranz-less, C4-type photosynthesis in *Hydrilla verticillata*. *Plant Physiology* **115**(4): 1681-1689.

Mann DG, Vanormelingen P. 2013. An inordinate fondness ? The number, distributions, and origins of diatom species. *Journal of Eukaryotic Microbiology* **60**(4): 414-420.

Matsuda Y, Nakajima K, Tachibana M. 2011. Recent progresses on the genetic basis of the regulation of CO_2 acquisition systems in response to CO_2 concentration. *Photosynthesis Research* **109**(1-3): 191-203.

McGinn PJ, Morel FMM. 2008. Expression and inhibition of the carboxylating and decarboxylating enzymes in the photosynthetic C4 pathway of marine diatoms. *Plant Physiology* **146**(1): 300-309.

Mekhalfi M, Puppo C, Avilan L, Lebrun R, Mansuelle P, Maberly SC, Gontero B. 2014. Glyceraldehyde-3-phosphate dehydrogenase is regulated by ferredoxin-NADP reductase in the diatom *Asterionella formosa*. *New Phytologist* **203**(2): 414-423.

Moustafa A, Beszteri B, Maier UG, Bowler C, Valentin K, Bhattacharya D. 2009. Genomic footprints of a cryptic plastid endosymbiosis in diatoms. *Science* **324**(5935): 1724-1726.

Mueller-Cajar O, Stotz M, Wendler P, Hartl FU, Bracher A, Hayer-Hartl M. 2011. Structure and function of the AAA+ protein CbbX, a red-type Rubisco activase. *Nature* **479**(7372): 194-199.

Nakajima K, Tanaka A, Matsuda Y. 2013. SLC4 family transporters in a marine diatom directly pump bicarbonate from seawater. *Proceedings of the National Academy of Sciences* **110**(5): 1767-1772.

Qu Z, Hartzell HC. 2008. Bestrophin Cl^- channels are highly permeable to HCO_3. *American Journal of Physiology-Cell Physiology* **294**(6): C1371-C1377.

Raven J. 2010. Inorganic carbon acquisition by eukaryotic algae: four current questions. *Photosynthesis Research* **106**(1-2): 123-134.

Raven JA, Giordano M, Beardall J, Maberly SC. 2012. Algal evolution in relation to atmospheric CO_2: carboxylases, carbon-concentrating mechanisms and carbon oxidation cycles. *Philosophical Transactions of the Royal Society B: Biological Sciences* **367**(1588): 493-507.

Reinfelder JR, Kraepiel AML, Morel FMM. 2000. Unicellular C4 photosynthesis in a marine diatom. *Nature* **407**(6807): 996-999.

Reinfelder JR, Milligan AJ, Morel FMM. 2004. The role of the C4 pathway in carbon accumulation and fixation in a marine diatom. *Plant Physiology* **135**(4): 2106-2111.

Reiskind JB, Bowes G. 1991. The role of phosphoenolpyruvate carboxykinase in a marine macroalga with C4-like photosynthetic characteristics. *Proceedings of the National Academy of Sciences of the United States of America* **88**(7): 2883-2887.

Reiskind JB, Seamon PT, Bowes G. 1988. Alternative methods of photosynthetic carbon assimilation in marine macroalgae. *Plant Physiology* **87**(3): 686-692.

Ritchie R. 2006. Consistent sets of spectrophotometric chlorophyll equations for acetone, methanol and ethanol solvents. *Photosynthesis Research* **89**(1): 27-41.

Roberts K, Granum E, Leegood R, Raven J. 2007a. Carbon acquisition by diatoms. *Photosynthesis Research* **93**(1-3): 79-88.

Roberts K, Granum E, Leegood RC, Raven JA. 2007b. C3 and C4 pathways of photosynthetic carbon assimilation in marine diatoms are under genetic, not environmental, control. *Plant Physiology* **145**(1): 230-235.

Sage RF. 2004. The evolution of C4 photosynthesis. *New Phytologist* **161**(2): 341-370.

Sakano K. 1998. Revision of biochemical pH-stat: Involvement of alternative pathway metabolisms. *Plant and Cell Physiology* **39**(5): 467-473.

Samukawa M, Shen C, Hopkinson B, Matsuda Y. 2014. Localization of putative carbonic anhydrases in the marine diatom, *Thalassiosira pseudonana*. *Photosynthesis Research* **121**(2-3): 235-249.

Sarthou G, Timmermans KR, Blain S, Tréguer P. 2005. Growth physiology and fate of diatoms in the ocean: a review. *Journal of Sea Research* **53**(1–2): 25-42.

Sims PA, Mann DG, Medlin LK. 2006. Evolution of the diatoms: insights from fossil, biological and molecular data. *Phycologia* **45**(4): 361-402.

Sorhannus U. 2007. A nuclear-encoded small-subunit ribosomal RNA timescale for diatom evolution. *Marine Micropaleontology* **65**(1–2): 1-12.

Spilling K, Ylostalo P, Simis S, Seppala J. 2015. Interaction effects of light, temperature and nutrient limitations (N, P and Si) on growth, stoichiometry and photosynthetic parameters of the cold-water diatom *Chaetoceros wighamii*. *PLoS One* **10**(5): e0126308.

Sültemeyer D, Klöck G, Kreuzberg K, Fock H. 1988. Photosynthesis and apparent affinity for dissolved inorganic carbon by cells and chloroplasts of *Chlamydomonas reinhardtii* grown at high and low CO_2 concentrations. *Planta* **176**(2): 256-260.

Tanaka R, Kikutani S, Mahardika A, Matsuda Y. 2014. Localization of enzymes relating to C4 organic acid metabolisms in the marine diatom, *Thalassiosira pseudonana*. *Photosynthesis Research* **121**(2-3): 251-263.

Tanaka Y, Nakatsuma D, Harada H, Ishida M, Matsuda Y. 2005. Localization of soluble β-carbonic anhydrase in the marine diatom *Phaeodactylum tricornutum*. Sorting to the chloroplast and cluster formation on the girdle lamellae. *Plant Physiology* **138**(1): 207-217.

Taylor AR, Brownlee C, Wheeler GL. 2012. Proton channels in algae: reasons to be excited. *Trends in Plant Science* **17**(11): 675-684.

Trimborn S, Wolf-Gladrow D, Richter K-U, Rost B. 2009. The effect of pCO_2 on carbon acquisition and intracellular assimilation in four marine diatoms. *Journal of Experimental Marine Biology and Ecology* **376**(1): 26-36.

Voznesenskaya EV, Franceschi VR, Kiirats O, Freitag H, Edwards GE. 2001. Kranz anatomy is not essential for terrestrial C4 plant photosynthesis. *Nature* **414**(6863): 543-546.

Weiss RF. 1974. Carbon dioxide in water and seawater: the solubility of a non-ideal gas. *Marine Chemistry* **2**(3): 203-215.

Whitney SM, Sharwood RE, Orr D, White SJ, Alonso H, Galmés J. 2011. Isoleucine 309 acts as a C4 catalytic switch that increases ribulose-1,5-bisphosphate carboxylase/oxygenase (rubisco) carboxylation rate in *Flaveria*. *Proceedings of the National Academy of Sciences of the United States of America* **108**(35): 14688-14693.

Wilbur KM, Anderson NG. 1948. Electrometric and colorimetric determination of carbonic anhydrase. *Journal of Biological Chemistry* **176**(1): 147-154.

Xu J, Zhang X, Ye N, Zheng Z, Mou S, Dong M, Xu D, Miao J. 2013. Activities of principal photosynthetic enzymes in green macroalga *Ulva linza*: functional implication of C4 pathway in CO_2 assimilation. *Science China Life Sciences* **56**(6): 571-580.

Xue J, Niu YF, Huang T, Yang WD, Liu JS, Li HY. 2015. Genetic improvement of the microalga *Phaeodactylum tricornutum* for boosting neutral lipid accumulation. *Metab Eng* **27**: 1-9.

Zhang Y, Yin L, Jiang H-S, Li W, Gontero B, Maberly SC. 2014. Biochemical and biophysical CO_2 concentrating mechanisms in two species of freshwater macrophyte within the genus *Ottelia* (Hydrocharitaceae). *Photosynthesis Research* **121**(2-3): 285-297.

642 **Figure legends**

643 **Fig. 1**. Growth of *T. pseudonana* and pH of culture at 400 ppm CO_2 (●), 20 000 ppm CO_2 (○)
644 and switched from 20 000 ppm to 50 ppm CO_2 after 60 hours (▼). (a) Growth followed using
645 optical density at 600 nm. (b) culture pH.

646

647 **Fig. 2**. Rate of net photosynthesis of *T. pseudonana* grown at 400 ppm or 20 000 ppm CO_2.
648 (a) Rate measured for 400 ppm cultures at pH 7 (●) or pH 8 (○) *vs* concentration of dissolved
649 inorganic carbon. (b) Modelled rate for 400 ppm cultures for combined pH values *vs*
650 concentration of CO_2. (c) Modelled rate for 400 ppm cultures for combined pH values vs
651 concentration of HCO_3^-. (d) Rate measured for 20 000 ppm cultures at pH 7 (●) or pH 8 (○) *vs*
652 concentration of dissolved inorganic carbon. (e) Modelled rate for 20 000 ppm cultures for
653 combined pH values *vs* concentration of CO_2. (f) Modelled rate for 20 000 ppm cultures for
654 combined pH values *vs* concentration of HCO_3^-. The kinetic parameters for the model are
655 shown in Table 2.

656

657 **Fig. 3.** Rate of net photosynthesis at pH 7 of *T. pseudonana* grown at 20 000 ppm CO_2 (●)
658 and then switched to 50 ppm CO_2 for 6 hours (○) or 12 hours (▼).The experimental data
659 were fitted to a slightly modified Michaelis-Menten equation that took into account the
660 compensation point for DIC, parameters are given in Table 1.

661

662 **Fig. 4**. Activities of partially CO_2-activated Rubisco, C4 enzymes and carbonic anhydrase in
663 *T. pseudonana* grown at 400 ppm CO_2 (black bars) and 20 000 ppm CO_2 (grey bars). Bars to
664 the left-hand side of the vertical line refer to the left-hand axis and *vice versa*. Error bars
665 represent one standard deviation. ***, $P<0.001$.

666

667 **Fig. 5**. Time course of enzyme activities after switching cultures from 20 000 ppm to 50 ppm
668 CO_2. (a) Activities of partially CO_2-activated Rubisco (○) and PEPCase (●). (b) Ratio of
669 PEPCase : Rubisco. (c) Activity of carbonic anhydrase. Error bars represent one standard
670 deviation.

671

Fig. 6. Effect of acetazolamide (0.4 mM) on the kinetics of carbon uptake at pH 7 for *T. pseudonana* grown at 400 ppm CO_2. Control (●) and treated cells (○) are shown.

Fig. 7. Activities of partially CO_2-activated Rubisco, C4 enzymes and carbonic anhydrase in *T. pseudonana* grown at 20 000 ppm CO_2 and switched to 50 ppm CO_2 for 24 hours (black bars) and then returned to 20 000 ppm CO_2 for 12 hours (grey bars). Bars to the left-hand side of the vertical line refer to the left-hand axis and *vice versa*. Error bars represent one standard deviation. NS, not significant ; **, $P<0.01$; ***, $P<0.001$.

684

685 Table 1. Kinetics of photosynthesis by *T. pseudonana* grown at different CO_2 concentrations and measured at different pH values and treated
686 with 0.4 mM AZA. Values are the mean with standard error in parentheses.

CO_2 (ppm)	pH	V_{net}^{max} (µmol O_2 h^{-1} mg^{-1} Chl*a*)	$K_{½}$ (µmol DIC L^{-1})	CP (µmol DIC L^{-1})	Slope (µmol O_2 h^{-1} mg^{-1} Chl*a* µmol^{-1} DIC L)	R^2
400	7	111 (3)	4.2 (0.9)	0.8 (0.2)	26 (6)	0.99
400	8	113 (3)	15.3 (1.6)	2.4 (0.4)	7 (1)	0.99
20 000	7	205 (17)	58.9 (22.6)	2.9 (5.9)	4 (1)	0.74
20 000	8	95 (8)	46.5 (19)	5.1 (4.7)	2 (1)	0.71
50 (6 h)	7	179 (5)	25.3 (3.6)	3.1(0.9)	7 (1)	0.95
50 (12 h)	7	156 (3)	13.3 (1.4)	1.8 (0.4)	12 (1)	0.97
400 + AZA	7	163 (7)	23.0 (4.2)	3.2 (0.9)	7 (1)	0.96

687

Table 2. Modelled kinetics of CO_2-dependent and HCO_3^--dependent photosynthesis by *T. pseudonana* grown at 400 or 20 000 ppm CO_2. Values are the mean with standard error of the estimate in parenthesis. Estimated rates as a percent of V_{net}^{max} calculated for 16 µM CO_2 and 2000 µM HCO_3^-. The raw data are shown in Fig. 2a,d and the outcomes of the models are shown in Fig. 2b,c,e,f.

	V_{net}^{max} (µmol mg^{-1} Chl*a* h^{-1})		$K_{½}$ (µmol L^{-1})		CP (µmol L^{-1})		Slope (µmol O_2 h^{-1} mg^{-1} Chl*a* µmol^{-1} L)		Percent of V_{net}^{max} under ambient		
CO_2 (ppm)	CO_2	HCO_3^-	CO_2	HCO_3^-	CO_2	HCO_3^-	CO_2	HCO_3^-	CO_2	HCO_3^-	R^2
400	85 (9)	27 (9)	0.4 (0.1)	2.7 (0.4)	0.0 (0.0)	7.5 (0.7)	296 (38)	42 (6)	98	100	0.92
20 000	202 (39)	0.0	3.8 (0.1)	-	0.0 (0.0)	-	53 (9)	-	60	-	0.60

- : not applicable as bicarbonate use is absent.

692

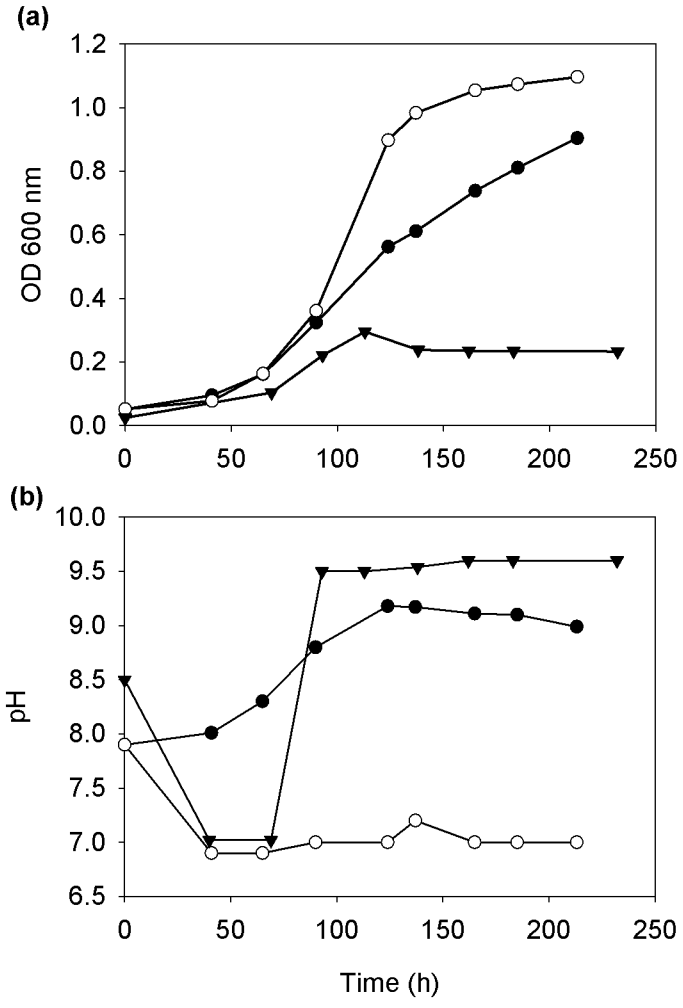
(a)
OD 600 nm
1.2
1.0
0.8
0.6
0.4
0.2
0.0
0
50
100
150
200
250
(b)
pH
10.0
9.5
9.0
8.5
8.0
7.5
7.0
6.5
0
50
100
150
200
250
Time (h)

Fig. 1

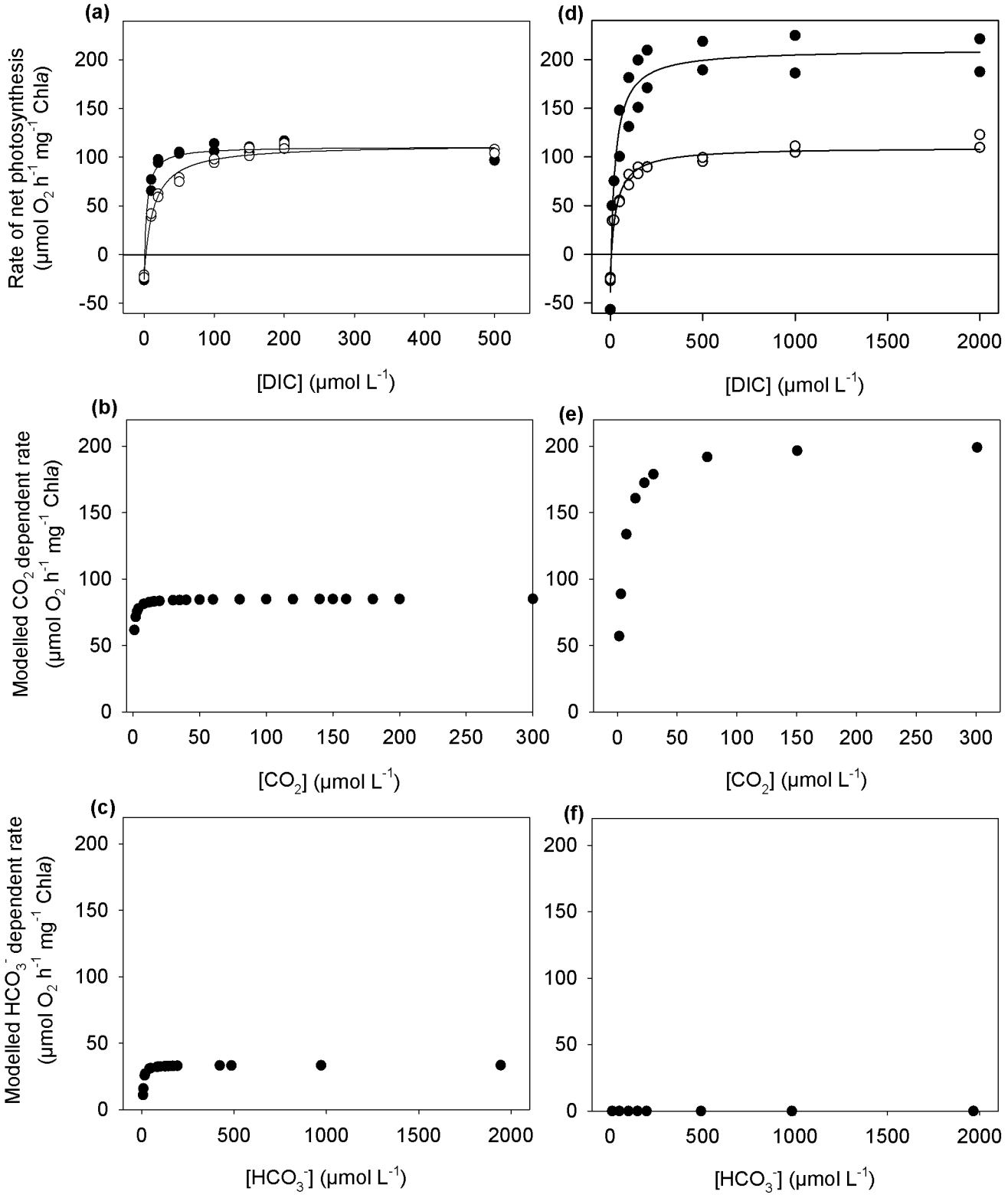
(a)
(d)
(b)
(e)
(c)
(f)
Rate of net photosynthesis (µmol O_2 h^{-1} mg^{-1} Chl*a*)
Modelled CO_2 dependent rate (µmol O_2 h^{-1} mg^{-1} Chl*a*)
Modelled HCO_3^- dependent rate (µmol O_2 h^{-1} mg^{-1} Chl*a*)
[DIC] (µmol L^{-1})
[CO_2] (µmol L^{-1})
[HCO_3^-] (µmol L^{-1})

Fig. 2

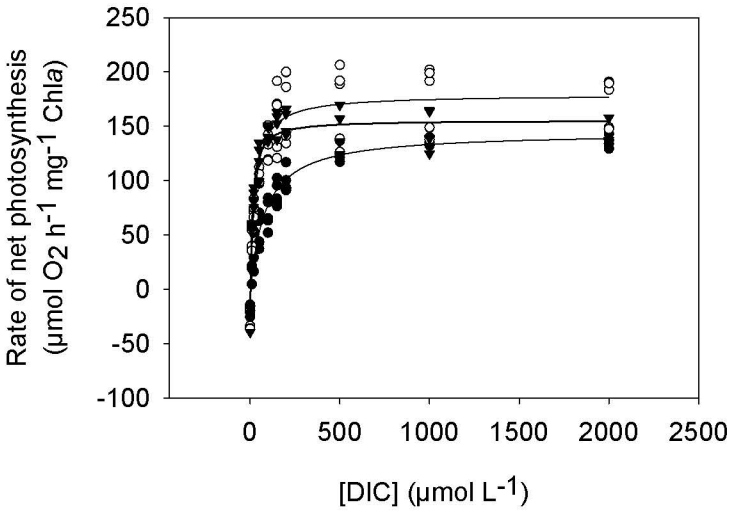
Rate of net photosynthesis
(µmol O2 h-1 mg-1 Chla)
250
200
150
100
50
0
-50
-100
0
500
1000
1500
2000
2500
[DIC] (µmol L-1)

Fig 3

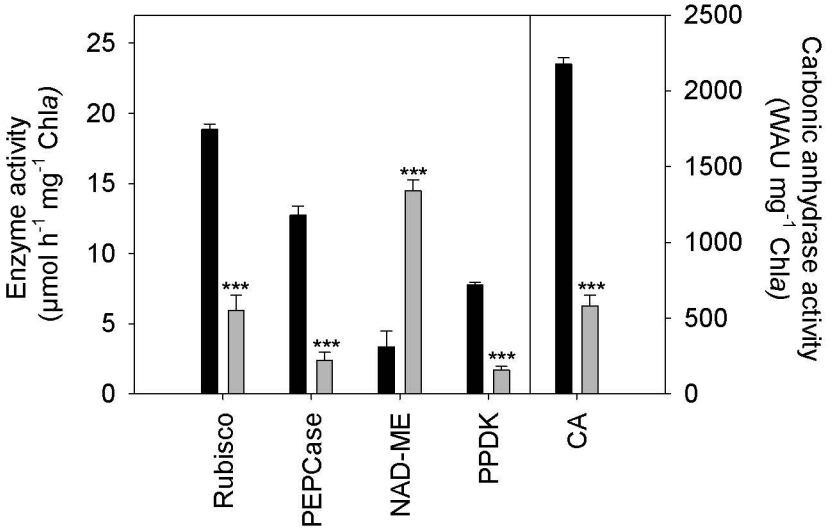
Enzyme activity
(μmol h-1 mg-1 Chla)
Carbonic anhydrase activity
(WAU mg-1 Chla)
0
5
10
15
20
25
0
500
1000
1500
2000
2500
***
***
***
***
***
Rubisco
PEPCase
NAD-ME
PPDK
CA

Fig. 4

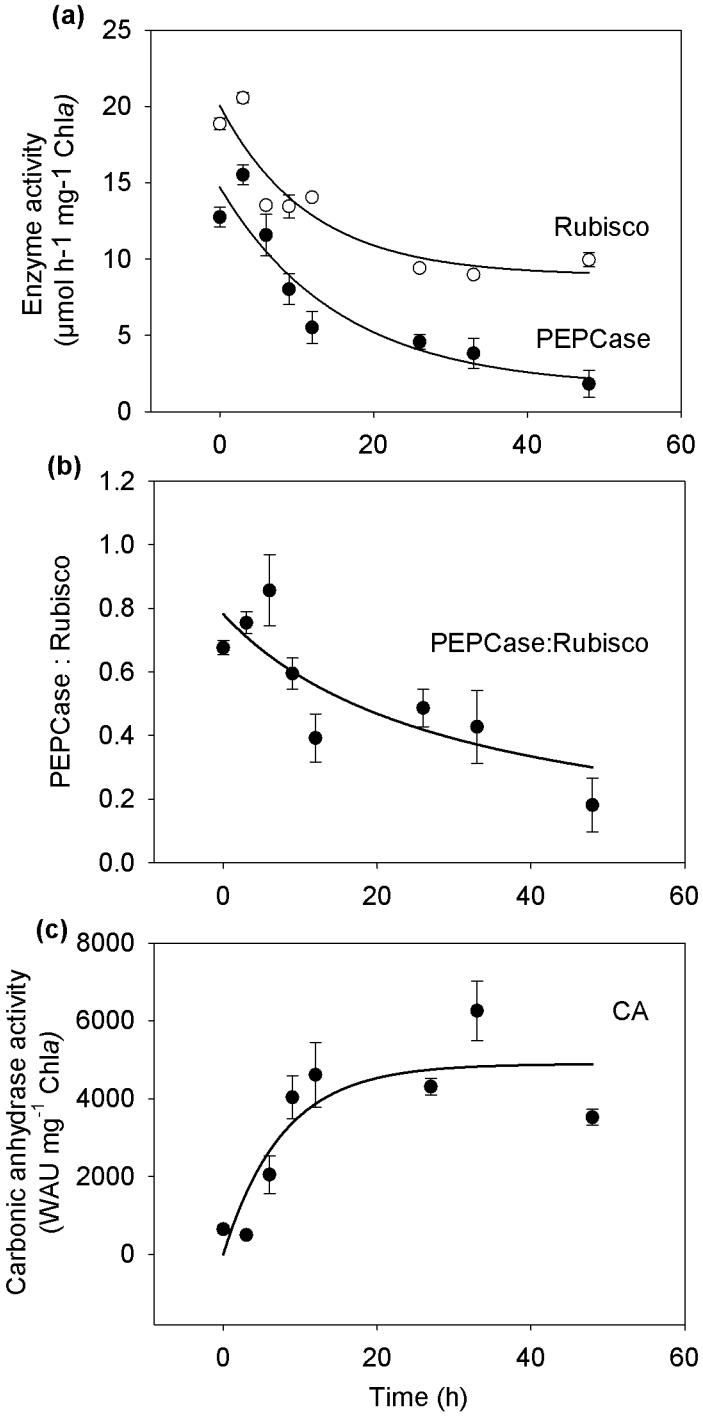
(a)
Enzyme activity (µmol h-1 mg-1 Chla)
Rubisco
PEPCase
(b)
PEPCase : Rubisco
PEPCase:Rubisco
(c)
Carbonic anhydrase activity (WAU mg-1 Chla)
CA
Time (h)

Fig. 5

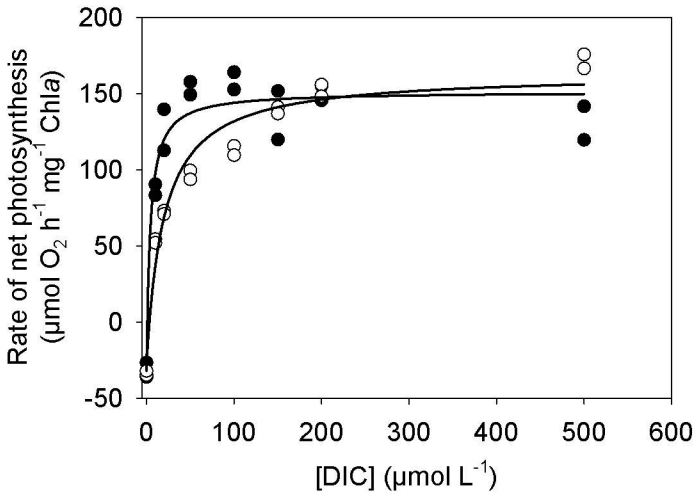
Rate of net photosynthesis
(µmol O_2 h^{-1} mg^{-1} Chla)
200
150
100
50
0
-50
0
100
200
300
400
500
600
[DIC] (µmol L^{-1})

Fig 6

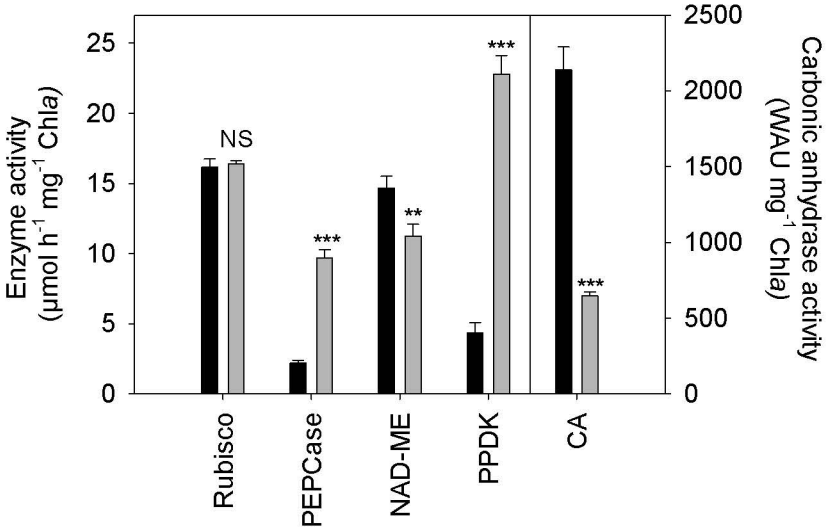
Enzyme activity
(µmol h-1 mg-1 Chla)
Carbonic anhydrase activity
(WAU mg-1 Chla)
25
20
15
10
5
0
2500
2000
1500
1000
500
0
NS
***
**
***
***
Rubisco
PEPCase
NAD-ME
PPDK
CA

Fig. 7